

## Facile Room Temperature Ion-Exchange Synthesis of $\text{Sn}^{2+}$ Incorporated Pyrochlore-Type Oxides and Their Photocatalytic Activities

S. Uma,\* Jyoti Singh, and Vaishali Thakral

*Materials Chemistry Group, Department of Chemistry, University of Delhi, Delhi-110007, India*

Received August 19, 2009

Ion-exchange reactions of aqueous  $\text{SnCl}_2 \cdot 2\text{H}_2\text{O}$  solutions with oxides such as  $\text{H}_2\text{Sb}_2\text{O}_6 \cdot 3.0\text{H}_2\text{O}$ ,  $\text{KSbWO}_6$ , and  $\text{KTaWO}_6 \cdot 1.0\text{H}_2\text{O}$  resulted in novel  $\text{Sn}^{2+}$  incorporated pyrochlore-type oxides under ambient conditions. Characterization of the  $\text{Sn}^{2+}$  exchanged products by powder X-ray diffraction, EDAX, thermogravimetric analysis, and chemical analysis yielded nominal compositions of  $\text{Sn}_{0.92}\text{Sb}_2\text{O}_6 \cdot 2.0\text{H}_2\text{O}$ ,  $\text{K}_{0.59}\text{Sn}_{0.20}\text{SbWO}_6 \cdot 1.0\text{H}_2\text{O}$ , and  $\text{K}_{0.58}\text{Sn}_{0.29}\text{TaWO}_6 \cdot 1.0\text{H}_2\text{O}$ . Diffuse reflectance spectra of the oxides incorporated with  $\text{Sn}^{2+}$  ions clearly exhibited red shifts from their respective parent oxides. The observed reduction in the band gaps to an extent of 0.9–1.6 eV was consistent with the  $\text{Sn}^{2+}$  ion-exchange, and indicated the upward shifting of the valence band resulting from the contribution of 5s band of  $\text{Sn}^{2+}$  to the O 2p band. Photocatalytic activities of the synthesized pyrochlore oxides were consistent with their electronic properties and decomposed methyl orange (MO) solutions under visible light. The pseudo first order rate constants of the oxides  $\text{Sn}_{0.92}\text{Sb}_2\text{O}_6 \cdot 2.0\text{H}_2\text{O}$  and  $\text{K}_{0.59}\text{Sn}_{0.20}\text{SbWO}_6 \cdot 1.0\text{H}_2\text{O}$  for the decomposition of MO solutions were found to be  $1.34 \text{ h}^{-1}$  and  $0.217 \text{ h}^{-1}$ , respectively, and almost a negligible MO decomposition was observed for  $\text{K}_{0.58}\text{Sn}_{0.29}\text{TaWO}_6 \cdot 1.0\text{H}_2\text{O}$ . The photocatalytic efficiencies of the oxides were found to be proportional to the rate of formation of  $\cdot\text{OH}$  radicals, which was found to vary in the order,  $\text{Sn}_{0.92}\text{Sb}_2\text{O}_6 \cdot 2.0\text{H}_2\text{O} > \text{K}_{0.59}\text{Sn}_{0.20}\text{SbWO}_6 \cdot 1.0\text{H}_2\text{O} > \text{K}_{0.58}\text{Sn}_{0.29}\text{TaWO}_6 \cdot 1.0\text{H}_2\text{O}$  as determined by the photoluminescence spectra using terephthalic acid.

### 1. Introduction

The chemistry of  $\text{Sn}^{2+}$  mixed metal oxides has been limited by the difficulties associated with the conventional solid state method of synthesis. The main disadvantage of the solid state synthesis of  $\text{Sn}^{2+}$  containing mixed metal oxides is the high temperature disproportionation of  $\text{Sn}^{2+}$  to  $\text{Sn}^{4+}$  and metallic Sn. Nevertheless, oxides of  $\text{Sn}^{2+}$  have continued to attract the researchers from the point of view of interesting structures and applications.  $\text{Sn}^{2+}$ , a lone pair cation, with the electronic configuration of  $4d^{10}5s^25p^0$  offers an environmentally attractive alternate to oxides containing  $\text{Pb}^{2+}$  cations. The first structurally characterized  $\text{Sn}^{2+}$  oxides were the tungsten bronzes of the type  $\text{Sn}_x\text{WO}_3$ .<sup>1</sup> Synthesis and single crystal structural determination were carried out subsequently for the low temperature  $\alpha$ - $\text{SnWO}_4$  (synthesized around 625 °C) and high temperature  $\beta$ - $\text{SnWO}_4$  (obtained by quenching from 670 °C) oxides.<sup>2,3</sup> Recently,  $\text{Sn}_2\text{WO}_5$  and  $\text{Sn}_3\text{WO}_6$  were synthesized and characterized<sup>4</sup> specifically to address the second-order-Jahn–Teller type structural distortions arising

by the presence of the lone pair  $\text{Sn}^{2+}$  cation along with the octahedrally coordinated  $d^0$  transition metal cation,  $\text{W}^{6+}$ . Interesting non-stoichiometric pyrochlore structure-type oxides of  $\text{Sn}^{2+}$  with other  $d^0$  transition metal cations such as  $\text{Nb}^{5+}$  and  $\text{Ta}^{5+}$  were known much earlier.<sup>5</sup> Invariably,  $\text{Sn}^{4+}$  was present, and the compositions were better identified as  $\text{Sn}_{2-x}^{2+}(\text{Sn}_y^{4+}\text{M}_{2-y}^{5+})\text{O}_{7-x-(y/2)}$  ( $\text{M} = \text{Nb}, \text{Ta}$ ).<sup>5</sup>

The structure of pyrochlore represented by the ideal formula  $\text{A}_2\text{B}_2\text{O}_7$  is versatile, and a wide variety of mixed metal oxides adopt this structure depending upon the choice of the metal cations A and B.<sup>6</sup> The novelty behind synthesizing  $\text{Sn}^{2+}$  containing pyrochlore structure type oxides has been to understand the local coordination environment of the lone pair  $\text{Sn}^{2+}$  cation, which is expected to occupy the high symmetrical ( $\bar{3}m$ ) position in these structures. Structural characterizations including X-ray diffraction and tin Mössbauer studies concluded that  $\text{Sn}^{2+}$  has deviated from the ideal  $\bar{3}m$  symmetry site resulting in an acentric structure leading to ferroelectricity.<sup>5</sup> Another interesting feature in these structures has been the variation in optical properties resulting from the contribution of Sn 5s band to the O 2p band in the construction of the valence band, especially in the presence of transition metal  $d^0$  ions. Both of the above-mentioned aspects

\*To whom correspondence should be addressed. E-mail: suma@chemistry.du.ac.in.

(1) Gier, T. E.; Pease, D. C.; Sleight, A. W.; Bither, T. A. *Inorg. Chem.* 1986, 25, 1646.

(2) Jeitschko, W.; Sleight, A. W. *Acta Crystallogr.* 1974, B 30, 2088.

(3) Jeitschko, W.; Sleight, A. W. *Acta Crystallogr.* 1972, B 28, 3174.

(4) Chang, H. Y.; Ok, K. M.; Kim, J. H.; Stoltzfus, M.; Woodward, P.; Halasyamani, P. S. *Inorg. Chem.* 2007, 46, 7005.

(5) Birchall, T.; Sleight, A. W. *J. Solid State Chem.* 1975, 13, 118.

(6) Subramanian, M. A.; Aravamudan, G.; Subba Rao, G. V. *Prog. Solid State Chem.* 1983, 15, 55.

have been exemplified in the recently<sup>7</sup> synthesized pyrochlores of the type  $\text{Sn}_2\text{TiNbO}_6\text{F}$ ,  $\text{Sn}_2\text{Ti}_{0.9}\text{Ta}_{1.1}(\text{O,F})_7$ ,  $\text{Sn}_2^{2+}(\text{Sn}_{0.25}^{4+}\text{-W}_{1.22}\text{Sc}_{0.53})\text{O}_{6.96}$ , and  $\text{Sn}_{1.4}^{2+}(\text{Sn}_{0.19}^{4+}\text{Ti}_{1.06}\text{W}_{0.75})\text{O}_{6.15}$ . Synthesis and single crystal structural characterization of  $\text{Sn}_2\text{TiO}_4$  isostructural with the low temperature form of  $\text{Pb}_3\text{O}_4$  has also been reported.<sup>8</sup>

Consistently, almost all except  $\text{Sn}_2\text{WO}_5$ , the rest of the  $\text{Sn}^{2+}$  oxides discussed above have been synthesized under closed evacuated conditions preferably in quartz ampules by the normal high temperature ( $> 600\text{ }^\circ\text{C}$ ), solid state preparation methods. The following few synthetic modifications have also been successfully demonstrated for synthesizing  $\text{Sn}^{2+}$  mixed metal oxides.  $\text{Sn}_2\text{WO}_5$  itself could be synthesized under mild hydrothermal conditions employing  $\text{SnO}$ ,  $\text{WO}_3$ ,  $\text{NaOH}$ , and  $\text{NH}_4\text{OH}$  around  $220\text{ }^\circ\text{C}$ .<sup>4</sup> Single crystals of pyrochlore tin-niobate,  $\text{Sn}_{1.4}(\text{Nb}_{1.8}\text{Sn}_{0.2})\text{O}_{6.3}$  has been prepared by heating a mixture of  $\text{NaNbO}_3$  with excess of  $\text{SnCl}_2$  at  $1000\text{ }^\circ\text{C}$  in a quartz tube under vacuum.<sup>9,10</sup>  $\text{SnTa}_2\text{O}_6$  with a threulite structure was obtained by reacting  $\text{KTaO}_3$  in molten  $\text{SnCl}_2$  around  $400\text{ }^\circ\text{C}$  under nitrogen atmosphere.<sup>11</sup> A very simple and significant preparative route has been the ion-exchange of alkali metal ( $\text{K}^+$ ,  $\text{Cs}^+$ ) ions from the layered metal oxides such as  $\text{KTiNbO}_5$ ,  $\text{K}_4\text{Nb}_6\text{O}_{17}$ ,  $\text{CsTi}_2\text{NbO}_7$ ,  $\text{K}_2\text{Ti}_4\text{O}_9$ ,  $\text{K}_2\text{Ti}_2\text{O}_5$ , and  $\text{Cs}_2\text{Ti}_6\text{O}_{13}$  by  $\text{Sn}^{2+}$  ions using acidic  $\text{SnCl}_2$  solutions under ambient conditions.<sup>12</sup> Microwave assisted solvothermal synthesis was also successful in preparing a pyrochlore-type compound  $\text{Sn}_{1.24}\text{Ti}_{1.94}\text{O}_{3.66}(\text{OH})_{1.5}\text{F}_{1.42}$ .<sup>13</sup>

Our interest to investigate  $\text{Sn}^{2+}$  containing mixed metal oxides originated from the fact that materials with suitable band gaps might exist for carrying out photocatalytic reactions under visible light. For example, the above-mentioned  $\text{Sn}^{2+}$  ion-exchanged layered metal oxides of titanium and niobium showed absorption bands in the visible region because of the band gap reduction of their alkali metal parent oxides containing niobium and titanium ions.<sup>12</sup>  $\text{Sn}^{2+}/\text{KTiNbO}_5$  and  $\text{Sn}^{2+}/\text{K}_4\text{Nb}_6\text{O}_{17}$  oxides showed photocatalytic activities for  $\text{H}_2$  evolution from an aqueous methanol solution under visible light irradiation. Two polymorphs ( $\alpha$  and  $\beta$ ) of the semiconductor  $\text{SnWO}_4$  exhibited good photocatalytic activity for the degradation of rhodamine B dye solution and also were able to produce  $\text{H}_2$  from an aqueous methanolic solution under visible light.<sup>14</sup> The role of  $\text{Sn}^{2+}$  in the band structure of  $\text{SnM}_2\text{O}_6$  and  $\text{Sn}_2\text{M}_2\text{O}_7$  ( $\text{M} = \text{Nb, Ta}$ ) and their photocatalytic activities have been investigated in detail.<sup>15</sup>  $\text{SnNb}_2\text{O}_6$  synthesized by the solid state method showed photocatalytic activity for  $\text{H}_2$  and  $\text{O}_2$  evolution from solutions having sacrificial agents (methanol and  $\text{Ag}^+$ ) under visible light irradiation. The negative shift of the valence band

caused by the presence of  $\text{Sn}^{2+}$ , narrowed the band gap to an extent of 1.0–1.8 eV, and this reduction in the band gap has been argued to be higher than those produced by the introduction of  $\text{Bi}^{3+}$  and  $\text{Ag}^+$  ions in other metal oxides.<sup>15</sup> We recently demonstrated that the ilmenite polymorph of  $\text{AgSbO}_3$  wherein the ion  $\text{Ag}^+$  coupled with a  $d^{10}$  electronic configuration ion such as  $\text{Sb}^{5+}$  could be utilized as an effective visible light photocatalyst for the decomposition of organic compounds such as methylene blue, rhodamine B, and 4-chlorophenol solutions.<sup>16</sup> Here, we explore the possibility of synthesizing mixed metal oxides containing  $\text{Sn}^{2+}$  and  $\text{Sb}^{5+}$  ions to study their visible light driven photocatalytic activities.

We focused mainly on soft chemical preparative routes because previous synthetic attempts which were made by heating the stoichiometric mixture of  $\text{SnO}_2$  and  $\text{Sb}_2\text{O}_3$  in sealed ampules did not result in phase pure ideal pyrochlore  $\text{Sn}_2\text{Sb}_2\text{O}_7$  oxides.<sup>6,17</sup> Antimony based hydrous mixed metal oxides with the pyrochlore structure have been studied extensively for applications in nuclear wastewater treatment because of their excellent ion-exchange capabilities toward several alkali and alkaline earth metal ions ( $\text{Na}^+$ ,  $\text{Rb}^+$ ,  $\text{Cs}^+$ ,  $\text{Mg}^{2+}$ ,  $\text{Ca}^{2+}$ ,  $\text{Sr}^{2+}$ ,  $\text{Ba}^{2+}$ )<sup>18</sup> and transition metal ions ( $\text{Co}^{2+}$ ,  $\text{Mn}^{2+}$ ,  $\text{Ni}^{2+}$ ).<sup>19</sup> In addition silver ion exchanged pyrochlore oxides were prepared by the reaction of antimonic acid and silver nitrate solution at room temperature.<sup>20,21</sup> However, until now, these pyrochlore based hydrated antimony oxides ( $\text{Sb}_2\text{O}_5 \cdot n\text{H}_2\text{O}$ ) have not been examined for the exchange of  $\text{Sn}^{2+}$  ions. First, hydrated antimony oxide  $\text{Sb}_2\text{O}_5 \cdot n\text{H}_2\text{O}$ <sup>20</sup> was selected to examine the exchange of  $\text{Sn}^{2+}$  ions with  $\text{H}^+$  ions under ambient conditions, targeting a pyrochlore type oxide containing  $\text{Sn}^{2+}$  and  $\text{Sb}^{5+}$  ions. Second, A-site deficient alkali metal pyrochlore oxides<sup>6</sup> such as  $\text{KSbWO}_6$ , and  $\text{KTaWO}_6 \cdot 1.0\text{H}_2\text{O}$  were chosen to study the extent and effect of incorporation of  $\text{Sn}^{2+}$  ions by simple ion-exchange reactions. In this article, we present the successful synthesis of  $\text{Sn}^{2+}$  incorporated pyrochlore-type mixed metal oxides by facile ion exchange process. Metal oxides obtained after ion-exchange were characterized by X-ray powder diffraction, scanning electron microscopy (SEM), and diffuse reflectance spectroscopy. Finally, the photocatalytic experiments were carried out to estimate the efficiency of these oxides for the decomposition of common organic dyes such as methyl orange (MO) solutions under UV and visible light irradiations. In addition, the formation of  $\cdot\text{OH}$  radicals under light irradiation of these oxides was studied by the photoluminescence (PL) technique using terephthalic acid (TA) as the probe.<sup>22–24</sup>

(7) Mizoguchi, H.; Wattiaux, A.; Kykneshi, R.; Tate, J.; Sleight, A. W.; Subramanian, M. A. *Mater. Res. Bull.* **2008**, *43*, 1943.

(8) Kumada, N.; Yonesaki, Y.; Takei, T.; Kinomura, N.; Wada, S. *Mater. Res. Bull.* **2009**, *44*, 1298.

(9) Cruz, L. P.; Savariault, J. M.; Rocha, J. *Acta Crystallogr.* **2001**, *C57*, 1001.

(10) Cruz, L. P.; Savariault, J. M.; Rocha, J.; Jumas, J.-C.; Pedrosa de Jesus, J. D. J. *Solid State Chem.* **2001**, *156*, 349.

(11) Mizoguchi, H.; Sleight, A. W.; Subramanian, M. A. *Mater. Res. Bull.* **2009**, *44*, 1022.

(12) Hosogi, Y.; Kato, H.; Kudo, A. *J. Phys. Chem. C* **2008**, *112*, 11678.

(13) Xie, Y.; Yin, S.; Yamane, H.; Hashimoto, T.; Machida, H.; Sato, T. *Chem. Mater.* **2008**, *20*, 4931.

(14) Cho, I.-S.; Kwak, C. H.; Kim, D. W.; Lee, S.; Hong, K. S. *J. Phys. Chem. C* **2009**, *113*, 10647.

(15) Hosogi, Y.; Shimodaira, Y.; Kato, H.; Kobayashi, H.; Kudo, A. *Chem. Mater.* **2008**, *20*, 1299.

(16) Singh, J.; Uma, S. *J. Phys. Chem. C* **2009**, *113*, 12483.

(17) Brisse, F.; Stewart, D. T.; Seidl, V.; Knop, O. *Can. J. Chem.* **1972**, *50*, 3648.

(18) Abe, M.; Itoh, T. *J. Inorg. Nucl. Chem.* **1980**, *42*, 1641. Baetsle, L. H.; Huys, D. J. *Inorg. Nucl. Chem.* **1968**, *30*, 639. Moller, T.; Clearfield, A.; Harjula, R. *Chem. Mater.* **2001**, *13*, 4767.

(19) Lefebvre, J.; Gaymard, F. C. R. *Acad. Sci. Paris* **1965**, *260*, 6911. Abe, M.; Itoh, T. *Bull. Chem. Soc. Jpn.* **1968**, *41*, 33. Abe, M.; Itoh, T. *Bull. Chem. Soc. Jpn.* **1968**, *41*, 2366.

(20) Zarbin, A. J. G.; Alves, O. L.; Amarilla, J. M.; Rojas, R. M.; Rojo, J. M. *Chem. Mater.* **1999**, *11*, 1652.

(21) Mizoguchi, H.; Eng, H. W.; Woodward, P. M. *Inorg. Chem.* **2004**, *43*, 1667.

(22) Hirakawa, T.; Nosaka, Y. *Langmuir* **2002**, *18*, 3247.

(23) Chen, Z.; Zhang, W.; Shao, Y.; Chen, T.; Sun, M.; Fu, X. *J. Phys. Chem. C* **2009**, *113*, 4433.

(24) Liu, G.; Wang, L. Z.; Sun, C. H.; Yan, X. X.; Wang, X. W.; Chen, Z. G.; Smith, S. C.; Cheng, H. M.; Lu, G. Q. *Chem. Mater.* **2009**, *21*, 1266–1274.

## 2. Experimental Section

**2.1. Synthesis.** Hydrated antimony oxide was prepared by the addition of water and  $\text{H}_2\text{O}_2$  to  $\text{Sb}_2\text{O}_3$  (99% Aldrich) followed by vigorous stirring and heating around  $90^\circ\text{C}$ .<sup>20</sup> Repeated water washings were done to obtain the creamy white solid, which was dried at room temperature and then utilized for the ion-exchange reaction. Other defect pyrochlore oxides  $\text{KSbWO}_6$ <sup>25</sup> and  $\text{KTaWO}_6 \cdot 1.0\text{H}_2\text{O}$ <sup>26</sup> were prepared by taking appropriate stoichiometric mixtures of the reactant carbonates or oxides such as  $\text{K}_2\text{CO}_3$  (99%, Ranbaxy),  $\text{WO}_3$  (99%, Aldrich),  $\text{Sb}_2\text{O}_3$  (99%, Aldrich),  $\text{Nb}_2\text{O}_5$  (99%, Aldrich), and  $\text{Ta}_2\text{O}_5$  (99%, Aldrich). The powders were homogenized and heated around  $850^\circ\text{C}$  for 12 to 24 h with an intermediate grinding. All the powders were white in color. After the structural verification by powder X-ray diffraction (PXRD), the parent pyrochlore oxides were ion-exchanged with a solution of  $\text{SnCl}_2 \cdot 2.0\text{H}_2\text{O}$  (99%, Aldrich) in acidic medium. Typically, 1 g of the powder was stirred with 100 mL of 0.1 M tin(II) chloride solution in hydrochloric acid at room temperature (around  $27^\circ\text{C}$ ). The colors of the powders changed instantaneously, and the stirring was continued for 12 h to ensure complete ion-exchange. The products after ion-exchange were washed with water and dried at room temperature. The excess of unexchanged tin present in the filtrate solutions were determined by EDTA back-titration.<sup>27</sup>

**2.2. Characterization.** The PXRD patterns were recorded using PANalytical X'pert Pro diffractometer employing  $\text{Cu K}\alpha$  radiation. The thermogravimetric analysis (TGA) was done on Perkin-Elmer (Pyris Diamond) and Shimadzu 60WS thermogravimetric analyzers in air atmosphere at the heating rate of  $10^\circ\text{C}/\text{minute}$  from 50 to  $800^\circ\text{C}$ . The SEM micrographs of the samples were recorded in JEOL 200 KeV instrument. The elemental compositions were determined using QUANTA 200 FEG (FEI Netherlands) Scanning Electron microscope with EDX attachment. UV-visible diffuse reflectance data were collected over the spectral range 200–1000 nm using Perkin-Elmer Lambda 35 scanning double beam spectrometer equipped with a 50 mm integrating sphere.  $\text{BaSO}_4$  was used as a reference. The data were transformed into absorbance with the Kubelka–Munk function.

**2.3. Photocatalytic Experiments.** Photocatalytic studies were carried out using a 450 W xenon arc lamp (Oriel, Newport, U.S.A.) along with a water filter to cut down IR radiation and glass cut off filters, Melles Griot-03FCG057 to permit only visible light ( $400\text{ nm} \leq \lambda \leq 800\text{ nm}$ ) and Melles Griot-03SWP602 to permit only UV light ( $\lambda \leq 400\text{ nm}$ ) radiations as desired. The experimental details of the photochemical reactor have been reported earlier.<sup>16</sup> A typical experiment of degradation was carried out as follows: 0.5 g of the catalyst was added to 150 mL of aqueous solution of MO with an initial concentration of  $15 \times 10^{-6}\text{ mol/L}$  for UV and visible irradiation experiments. Prior to irradiation, the suspension of the catalyst and dye solution was stirred in dark for 30 to 60 min, so as to reach the equilibrium adsorption. Five milliliter aliquots were pipetted out periodically from the reaction mixture. The solutions were centrifuged, and the concentration of the solutions was determined by measuring the maximum absorbance ( $\lambda_{\text{max}} = 460\text{ nm}$ ). The production of  $\cdot\text{OH}$  radicals under visible irradiation was carried out by the PL technique using TA as the probe. TA readily reacts with  $\cdot\text{OH}$  radicals to give the product 2-hydroxyterephthalic acid which has a PL emission around 426 nm. The excitation was carried out around 312 nm, and the increase in the photoluminescent intensity of 2-hydroxyterephthalic acid is directly proportional to the  $\cdot\text{OH}$  radicals

generated.<sup>22–24</sup> About 0.1 g of the  $\text{Sn}^{2+}$  containing oxides were taken with 50 mL of TA solution (3 mmol) and NaOH (10 mmol). Five milliliter aliquots were sampled out at regular intervals after visible light irradiation, and the PL intensities were measured using VARIAN Cary Eclipse spectrofluorometer.

## 3. Results and Discussion

**3.1. Synthesis and Structure.** Among the ternary metal oxides, pyrochlores have the general formula  $\text{A}_2\text{B}_2\text{O}_7$  or  $\text{A}_2\text{B}_2\text{O}_6\text{O}'$ . The space group is  $Fd\bar{3}m$ , and the symmetry is usually cubic. The structure<sup>6</sup> is built from corner sharing  $\text{BO}_6$  octahedra and an interpenetrating  $\text{A}_2\text{O}'$  chain. The B cation is thus six coordinated, and the A cations normally have eight coordinated O atoms, six oxygens from  $\text{BO}_6$  octahedra, and two  $\text{O}'$  atoms from  $\text{A}_2\text{O}'$  chains. The pyrochlore structure is known to exist with vacancies at the A and  $\text{O}'$  sites giving defect pyrochlores. Such defect pyrochlores were known to exhibit interesting ion-exchange properties because of the mobility of  $\text{A}^+$  ions coupled with the rigidity of the framework formed by octahedral  $\text{BO}_6$  units. Various metal ion substitutions at the A and/or B sites have been investigated in detail to achieve specific tuning of the ion-exchange properties of the antimonates, antimony silicates, antimony titanates, and titanium tungstates based materials with defect pyrochlore structure.<sup>18–20,28</sup> These studies were intended to produce pyrochlore oxides capable of exchanging selective metal ions such as  $\text{Sr}^{2+}$  from nuclear waste effluents. In the present study, we focused on the A site ion-exchange to synthesize novel  $\text{Sn}^{2+}$  incorporation in the pyrochlore oxides that otherwise requires inert conditions.

The parent compounds adopting the defect pyrochlore structures were initially characterized. Under the experimental conditions employed, the hydrated antimonite oxide was found to be  $\text{H}_2\text{Sb}_2\text{O}_6 \cdot 3.0\text{H}_2\text{O}$  ( $\text{Sb}_2\text{O}_5 \cdot 4.0\text{H}_2\text{O}$ ) from thermo gravimetric analysis<sup>29</sup> (Supporting Information, Figure S1). The PXRD (Figure 1) confirmed the formation of a pyrochlore-type structure,<sup>20</sup> and the reflections matched well with the reported values, Powder Diffraction File (PDF) No. 84–0303. Both  $\text{KSbWO}_6$  and  $\text{KTaWO}_6 \cdot 1.0\text{H}_2\text{O}$  were prepared by the solid state reaction and the TGA confirmed the presence of water only in the latter (Supporting Information, Figure S1). PXRD patterns (Figure 2) and the lattice dimensions were similar to those reported for  $\text{KSbWO}_6$ <sup>25</sup> (PDF No. 25–0620) and  $\text{KTaWO}_6 \cdot 1.0\text{H}_2\text{O}$ <sup>26</sup> (PDF No. 74–1599).

Aqueous ion-exchange of pyrochlore-type oxides  $\text{H}_2\text{Sb}_2\text{O}_6 \cdot 3.0\text{H}_2\text{O}$ ,  $\text{KSbWO}_6$  and  $\text{KTaWO}_6 \cdot 1.0\text{H}_2\text{O}$  with  $\text{SnCl}_2 \cdot 2.0\text{H}_2\text{O}$  solutions at room temperature was sufficient to incorporate  $\text{Sn}^{2+}$  ions in these oxides. The SEM of the ion-exchanged powders along with their parent pyrochlore oxides revealed the formation of uniform crystallites in the micrometer range (Supporting Information, Figures S2 and S3). The images clearly indicated that there was no change in the morphology of the oxides before and after  $\text{Sn}^{2+}$  exchange. Exchange of  $\text{Sn}^{2+}$  ions for the protons in antimonite acid were evident from the instantaneous formation of shiny bright orange colored product during the

(25) Michel, C.; Groult, D.; Raveau, B. *Mater. Res. Bull.* **1973**, *8*, 201.

(26) Darriet, B.; Rat, M.; Galy, J.; Hagemmuller, P. *Mater. Res. Bull.* **1971**, *6*, 1305.

(27) Vogel, A. I. *Textbook of Quantitative Chemical Analysis*; Longman Group Ltd.: Harlow, U.K., 1989.

(28) Moller, T.; Clearfield, A.; Harjula, R. *Microporous Mesoporous Mater.* **2002**, *54*, 187.

(29) Ozawa, K.; Wang, J.; Ye, J.; Sakka, Y.; Amano, M. *Chem. Mater.* **2003**, *15*, 928.

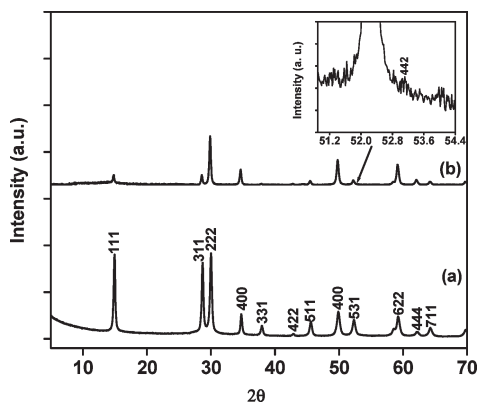


**Figure 1.** PXRD patterns of (a)  $\text{H}_2\text{Sb}_2\text{O}_6 \cdot 3.0\text{H}_2\text{O}$  and (b)  $\text{Sn}_{0.92}\text{Sb}_2\text{O}_6 \cdot 2.0\text{H}_2\text{O}$ . Inset shows the forbidden reflection 442 observed in  $\text{Sn}_{0.92}\text{Sb}_2\text{O}_6 \cdot 2.0\text{H}_2\text{O}$ .

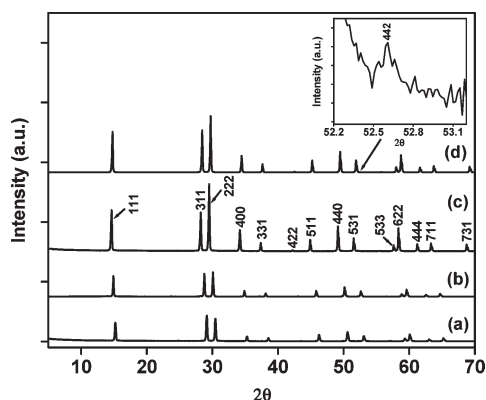


**Figure 2.** PXRD patterns of (a)  $\text{KSbWO}_6$ , (b)  $\text{K}_{0.59}\text{Sn}_{0.20}\text{SbWO}_6 \cdot 1.0\text{H}_2\text{O}$ , (c)  $\text{KTaWO}_6 \cdot 1.0\text{H}_2\text{O}$ , and (d)  $\text{K}_{0.58}\text{Sn}_{0.29}\text{TaWO}_6 \cdot 1.0\text{H}_2\text{O}$ . Inset shows the forbidden reflection 442 observed in  $\text{K}_{0.58}\text{Sn}_{0.29}\text{TaWO}_6 \cdot 1.0\text{H}_2\text{O}$ .

ion-exchange reaction (inset in Figure 3). Similarly, yellow and lemon yellow powders were obtained by the replacement of  $\text{K}^+$  by  $\text{Sn}^{2+}$  ions from  $\text{KSbWO}_6$  and  $\text{KTaWO}_6 \cdot 1.0\text{H}_2\text{O}$ , respectively (insets in Figures 4 and 5). Furthermore, flame photometric analysis of the filtrate obtained after ion-exchange confirmed the presence of replaced potassium ions. In all of the above ion-exchange reactions, the complexometric titration of the filtrate was carried out to estimate the excess  $\text{Sn}^{2+}$  ions and thereby the amounts of incorporated  $\text{Sn}^{2+}$  ions in the products were deduced. These results agreed well with the compositions that were obtained from the Energy Dispersive X-ray analysis (EDAX) of the samples (Supporting Information, Figure S4) and are summarized in Table 1. The extent of water introduced in the products was also estimated from TGA (Supporting Information, Figure S5) and are listed in Table 1. Thus, the compositions for the ion-exchanged products were identified to be  $\text{Sn}_{0.92}\text{Sb}_2\text{O}_6 \cdot 2.0\text{H}_2\text{O}$ ,  $\text{K}_{0.59}\text{Sn}_{0.20}\text{SbWO}_6 \cdot 1.0\text{H}_2\text{O}$ , and  $\text{K}_{0.58}\text{Sn}_{0.29}\text{TaWO}_6 \cdot 1.0\text{H}_2\text{O}$  (Table 1). The existence of  $\text{Sn}^{2+}$  and  $\text{Sb}^{3+}$  ions in  $\text{Sn}_{0.92}\text{Sb}_2\text{O}_6 \cdot 2.0\text{H}_2\text{O}$  is significant, unlike the solid state preparations under vacuum, where even the reaction between 400 and 700 °C of  $\text{SnO}_2$  either with  $\text{Sb}_2\text{O}_3$  or with antimonous acid did not yield any pyrochlore related product.<sup>17</sup> It is also relevant to mention that the  $\text{Sn}^{2+}$  incorporated oxides also have the defect pyrochlore structure of their parent oxides with vacancies at the A and O' sites. If we consider the charge balance of the product compositions

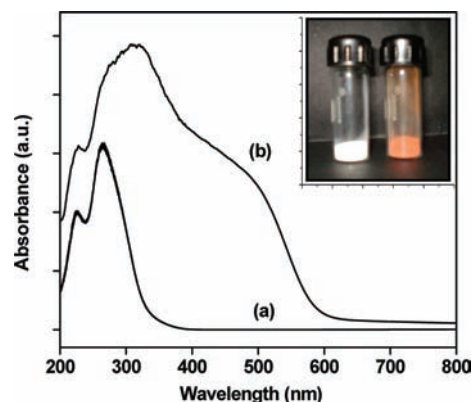


**Figure 3.** UV-visible diffuse reflectance spectra of (a)  $\text{H}_2\text{Sb}_2\text{O}_6 \cdot 3.0\text{H}_2\text{O}$  and (b)  $\text{Sn}_{0.92}\text{Sb}_2\text{O}_6 \cdot 2.0\text{H}_2\text{O}$ . Inset shows the respective samples.

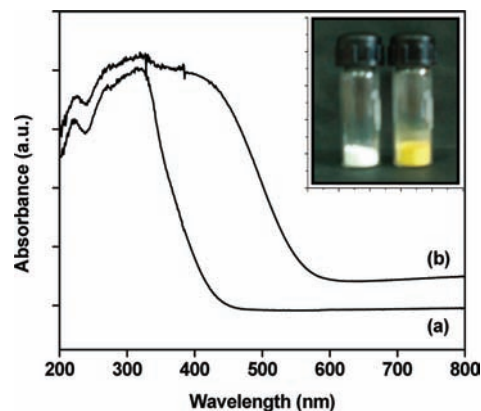


**Figure 4.** UV-visible diffuse reflectance spectra of (a)  $\text{KSbWO}_6$  and (b)  $\text{K}_{0.59}\text{Sn}_{0.20}\text{SbWO}_6 \cdot 1.0\text{H}_2\text{O}$ . Inset shows the respective samples.

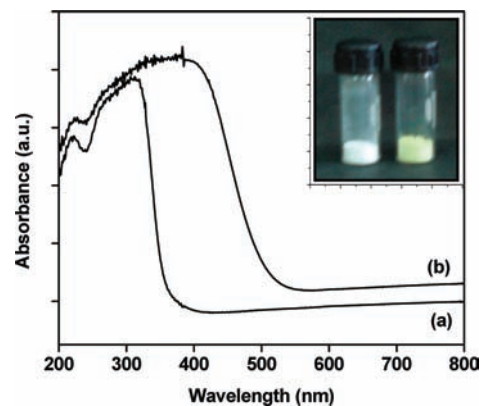


**Figure 5.** UV-visible diffuse reflectance spectra of (a)  $\text{KTaWO}_6 \cdot 1.0\text{H}_2\text{O}$  and (b)  $\text{K}_{0.58}\text{Sn}_{0.29}\text{TaWO}_6 \cdot 1.0\text{H}_2\text{O}$ . Inset shows the respective samples.

(Table 1), then for instance, in the case of  $\text{Sn}_{0.92}\text{Sb}_2\text{O}_6 \cdot 2.0\text{H}_2\text{O}$ , a Sn/Sb ratio of about 1:2 was obtained from both the EDAX elemental analysis and the complexometric titration. As a result of the replacement of two protons from  $\text{H}_2\text{Sb}_2\text{O}_6 \cdot 3.0\text{H}_2\text{O}$  by nearly one  $\text{Sn}^{2+}$  ion, the charge balance is obtained with the formation of an A-site deficient ( $\text{AB}_2\text{O}_6$ ) pyrochlore oxide.<sup>6</sup> Similar has been the situation with  $\text{K}_{0.59}\text{Sn}_{0.20}\text{SbWO}_6 \cdot 1.0\text{H}_2\text{O}$ , wherein the possibility of A-site deficiency occurs, while keeping the charge balanced with an oxygen content of six. Lastly, in the case of  $\text{K}_{0.58}\text{Sn}_{0.29}\text{TaWO}_6 \cdot 1.0\text{H}_2\text{O}$ , still the possibility of A-site

**Table 1.** Compositions of the Sn<sup>2+</sup> Pyrochlore Oxides As Determined by Various Analytical Techniques

S. no.	experiment	water content from TGA <sup>a</sup>	incorporated amount of Sn <sup>2+</sup> from complexometric titration <sup>b</sup>	elemental analysis from EDAX <sup>b</sup>	product composition
1.	H <sub>2</sub> Sb <sub>2</sub> O <sub>6</sub> ·3.0H <sub>2</sub> O + SnCl <sub>2</sub> ·2H <sub>2</sub> O	2.0	Sn/Sb = 0.92:2.0	Sn/Sb = 1.08:2.0	Sn <sub>0.92</sub> Sb <sub>2</sub> O <sub>6</sub> ·2.0H <sub>2</sub> O
2.	KSbWO <sub>6</sub> + SnCl <sub>2</sub> ·2H <sub>2</sub> O	1.0	Sn/(SbW) = 0.20:2.0	Sn/(SbW) = 0.15:2.0	K <sub>0.59</sub> Sn <sub>0.20</sub> SbWO <sub>6</sub> ·1.0H <sub>2</sub> O
3.	KTaWO <sub>6</sub> ·1.0H <sub>2</sub> O + SnCl <sub>2</sub> ·2H <sub>2</sub> O	1.0	Sn/(TaW) = 0.29:2.0	Sn/(TaW) = 0.29:2.0	K <sub>0.58</sub> Sn <sub>0.29</sub> TaWO <sub>6</sub> ·1.0H <sub>2</sub> O

<sup>a</sup> Water content calculated from the weight loss observed in TGA until ≤ 500 °C. <sup>b</sup> Fixed B cation (Sb, Ta, and W) content.

deficiency remains, but the charge of the ions in the A-site might force the oxygen content to be slightly higher (6.09 instead of 6.00). Finally, other additional probabilities such as the presence of a small amount of protons along with Sn<sup>2+</sup> ions in the exchanged products and the oxidation of a small amount of Sn<sup>2+</sup> to Sn<sup>4+</sup> ions during the exchange reactions may not be completely excluded.<sup>12</sup>

PXRD patterns (Figures 1 and 2) of the Sn<sup>2+</sup> containing pyrochlore-type oxides confirmed that the structure is intact with changes in the lattice parameters alone. The refined cubic unit cell dimensions obtained were  $a = 10.357(2)$  Å for Sn<sub>0.92</sub>Sb<sub>2</sub>O<sub>6</sub>·2.0H<sub>2</sub>O as compared to the parent antimonite oxide ( $a = 10.363(1)$  Å). Similarly, the unit cell parameters of KSbWO<sub>6</sub> and K<sub>0.59</sub>Sn<sub>0.20</sub>SbWO<sub>6</sub>·1.0H<sub>2</sub>O were  $a = 10.243(4)$  Å and  $a = 10.279(5)$  Å and the corresponding parameters of KTaWO<sub>6</sub>·1.0H<sub>2</sub>O and K<sub>0.58</sub>Sn<sub>0.29</sub>TaWO<sub>6</sub>·1.0H<sub>2</sub>O were found to be  $a = 10.475(3)$  Å and  $a = 10.451(2)$  Å. The observed changes in the lattice parameters were due to the small deviation of the  $d$  values that occurred during the Sn<sup>2+</sup> ion-exchange reactions. For example, the  $d$  values for the (400) reflections were 2.5812 Å (H<sub>2</sub>Sb<sub>2</sub>O<sub>6</sub>·3.0H<sub>2</sub>O), 2.5874 Å (Sn<sub>0.92</sub>Sb<sub>2</sub>O<sub>6</sub>·2.0H<sub>2</sub>O), 2.5421 Å (KSbWO<sub>6</sub>), and 2.5700 Å (K<sub>0.59</sub>Sn<sub>0.20</sub>SbWO<sub>6</sub>·1.0H<sub>2</sub>O). During the ion-exchange reactions of these mentioned pyrochlore oxides the products formations were accompanied by the incorporation of Sn<sup>2+</sup> ions along with the changes in the amount of their water of hydration. Introduction of Sn<sup>2+</sup> (ionic radius of Sn<sup>2+</sup>(VIII) = 1.36 Å)<sup>30,31</sup> in the eight coordinated site of the pyrochlore structure essentially would decrease the lattice parameters, while the increase in the amount of water of hydration would increase the lattice parameters of the products.<sup>6</sup> The combined effect was responsible for the observed variations in the lattice parameters of Sn<sub>0.92</sub>Sb<sub>2</sub>O<sub>6</sub>·2.0H<sub>2</sub>O and K<sub>0.59</sub>Sn<sub>0.20</sub>SbWO<sub>6</sub>·1.0H<sub>2</sub>O oxides as compared to their parent pyrochlore oxides. While in the case of KTaWO<sub>6</sub>·1.0H<sub>2</sub>O and K<sub>0.58</sub>Sn<sub>0.29</sub>TaWO<sub>6</sub>·1.0H<sub>2</sub>O, the water of hydration has not changed and the observed decrease ( $d$  value for the (400) reflection changed from 2.6200 Å in the parent to 2.6006 Å in the product) in the lattice parameters truly reflected the incorporation of smaller sized Sn<sup>2+</sup> (ionic radius of Sn<sup>2+</sup>(VIII) = 1.36 Å) ions replacing the bigger K<sup>+</sup> (ionic radius of K<sup>+</sup>(VIII) = 1.65 Å) ions.<sup>30,31</sup> Although the observed X-ray diffraction patterns indicated the formation of pyrochlore-type structure, (space group  $Fd\bar{3}m$ ) the presence of forbidden reflections such as 442, (Figures 1 and 2) pointed out to the deviation that arises because of the shifting of Sn<sup>2+</sup> ions from its ideal  $\bar{3}m$  site position.<sup>5,7</sup>

**3.2. Optical Properties.** Diffuse reflectance spectra of pyrochlore oxides before and after Sn<sup>2+</sup> ion-exchange are

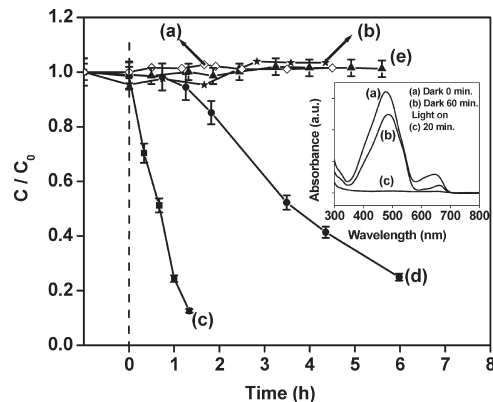


**Figure 6.** Photocatalytic decomposition of MO as indicated by the concentration ( $C_0$  is the initial concentration and  $C$  is the concentration at any time,  $t$ ). (a) MO blank, (b) MO on Sn<sub>0.92</sub>Sb<sub>2</sub>O<sub>6</sub>·2.0H<sub>2</sub>O in the absence of visible light, (c) MO on Sn<sub>0.92</sub>Sb<sub>2</sub>O<sub>6</sub>·2.0H<sub>2</sub>O under visible light irradiation, (d) MO on K<sub>0.59</sub>Sn<sub>0.20</sub>SbWO<sub>6</sub>·1.0H<sub>2</sub>O under visible light irradiation, and (e) MO on K<sub>0.58</sub>Sn<sub>0.29</sub>TaWO<sub>6</sub>·1.0H<sub>2</sub>O under visible light irradiation. Inset shows the absorption changes at 460 nm of MO solutions under UV light irradiation over Sn<sub>0.92</sub>Sb<sub>2</sub>O<sub>6</sub>·2.0H<sub>2</sub>O.

shown in Figures 3–5. Clearly the band gaps, after the introduction of Sn<sup>2+</sup>, have decreased considerably as observed from the red shifts of the absorption bands. The observed energy gaps for creamy white hydrated antimonite oxide and the orange Sn<sup>2+</sup> exchanged pyrochlore oxide, Sn<sub>0.92</sub>Sb<sub>2</sub>O<sub>6</sub>·2.0H<sub>2</sub>O were 3.64 and 2.02 eV, respectively (Figure 3). Also, KSbWO<sub>6</sub> (3.18 eV) and KTaWO<sub>6</sub>·1.0H<sub>2</sub>O (3.55 eV) showed band gap reduction after Sn<sup>2+</sup> incorporation and were found to be 2.3 eV for K<sub>0.59</sub>Sn<sub>0.20</sub>SbWO<sub>6</sub>·1.0H<sub>2</sub>O and 2.58 eV for K<sub>0.58</sub>Sn<sub>0.29</sub>TaWO<sub>6</sub>·1.0H<sub>2</sub>O (Figures 4 and 5). The band gap decrease, arising because of the contribution of 5s band from Sn<sup>2+</sup> to the O 2p band in the formation of the valence band has been well established in many of the reported Sn<sup>2+</sup> mixed metal oxides.<sup>5,7,12–15</sup> Narrowing of the band gap to 1.2 eV was noticed between KTiNbO<sub>5</sub> and Sn<sup>2+</sup> exchanged Sn<sub>0.475</sub>K<sub>0.05</sub>TiNbO<sub>5</sub>.<sup>12</sup> Band gap reduction of 1.4 eV was found between Ca<sub>2</sub>Ta<sub>2</sub>O<sub>7</sub> (4.4 eV) and Sn<sub>2</sub>Ta<sub>2</sub>O<sub>7</sub> (3.0 eV), and the band structure calculations revealed the contribution of Sn 5s orbitals to the valence band.<sup>15</sup> In the present case, among the three synthesized pyrochlore oxides, Sn<sub>0.92</sub>Sb<sub>2</sub>O<sub>6</sub>·2.0H<sub>2</sub>O with the highest amount of Sn<sup>2+</sup> incorporation showed a substantial decrease in the band gap as evidenced from a slightly broader absorption edge, and the remaining two oxides K<sub>0.59</sub>Sn<sub>0.20</sub>SbWO<sub>6</sub>·1.0H<sub>2</sub>O and K<sub>0.58</sub>Sn<sub>0.29</sub>TaWO<sub>6</sub>·1.0H<sub>2</sub>O, with less incorporated Sn<sup>2+</sup> content also showed appreciable and consistent decrease in their band gaps as shown by steeper absorption edges (Figures 3–5). The Sn<sup>2+</sup> pyrochlore oxides that were synthesized by ion-exchange in the present study, Sn<sub>0.92</sub>Sb<sub>2</sub>O<sub>6</sub>·2.0H<sub>2</sub>O, K<sub>0.59</sub>Sn<sub>0.20</sub>SbWO<sub>6</sub>·1.0H<sub>2</sub>O, and K<sub>0.58</sub>Sn<sub>0.29</sub>TaWO<sub>6</sub>·1.0H<sub>2</sub>O

(30) Muller O.; Roy, R. *The Major Ternary Structural Families*; Springer-Verlag: New York, 1974.

(31) Shannon, R. D.; Prewitt, C. T. *Acta Crystallogr.* **1969**, *B25*, 925. Shannon, R. D.; Prewitt, C. T. *Acta Crystallogr.* **1970**, *B26*, 1046.

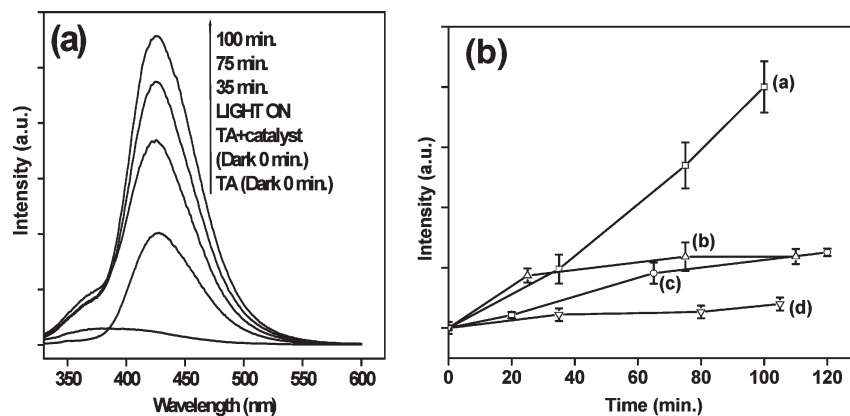


**Figure 7.** (a)  $\cdot\text{OH}$ -trapping PL spectra of  $\text{Sn}_{0.92}\text{Sb}_2\text{O}_6 \cdot 2.0\text{H}_2\text{O}$  in solution of TA at room temperature (ex, 312 nm; em, 426 nm) and (b) plot of the induced fluorescence intensity at 426 nm against irradiation time under visible light for (a)  $\text{Sn}_{0.92}\text{Sb}_2\text{O}_6 \cdot 2.0\text{H}_2\text{O}$ , (b)  $\text{K}_{0.59}\text{Sn}_{0.20}\text{SbWO}_6 \cdot 1.0\text{H}_2\text{O}$ , (c)  $\text{K}_{0.58}\text{Sn}_{0.29}\text{TaWO}_6 \cdot 1.0\text{H}_2\text{O}$ , and (d)  $\text{Sn}_{0.92}\text{Sb}_2\text{O}_6 \cdot 2.0\text{H}_2\text{O}$  in the dark.

showed efficient absorption in the UV region along with extended visible absorption (up to 550–600 nm), suggesting that these oxides might be potentially visible and/or UV photocatalysts. The absorption in the visible light region of these pyrochlores were possible mostly because of the transition from the valence band composed of Sn 5s and O 2p orbitals to the conduction band having the contribution mostly from the appropriate valence orbitals of the B site cations (Sb, Ta and W).<sup>15</sup>

**3.3. Photocatalytic Properties.** Degradation of MO was investigated under visible light ( $400 \text{ nm} \leq \lambda \leq 800 \text{ nm}$ ). Figure 6 showed the rates of decompositions of MO under visible light irradiation. Gradual disappearance of the dye solutions were observed, and concentrations were followed by the decrease in the absorbance around  $\lambda = 460 \text{ nm}$ . We applied the pseudo first order model of the photodegradation process to quantify the reaction kinetics and calculated the pseudo first order rate constants ( $k$ ) using the equation,  $\ln(C_0/C) = kt$ , where  $C_0$  and  $C$  are the concentrations of MO solution, respectively, at time 0 and  $t$ .<sup>32,33</sup>  $\text{Sn}_{0.92}\text{Sb}_2\text{O}_6 \cdot 2.0\text{H}_2\text{O}$  showed the highest decomposition rate under visible irradiation with a pseudo first order rate constant of  $1.34 \text{ h}^{-1}$ , and the pyrochlore oxide decomposed MO solutions much faster with an observed pseudo first order rate constant of  $5.03 \text{ h}^{-1}$  under UV irradiation (Inset in Figure 6).  $\text{K}_{0.59}\text{Sn}_{0.20}\text{SbWO}_6 \cdot 1.0\text{H}_2\text{O}$  exhibited a much lower activity with a pseudo first order rate constant of  $0.217 \text{ h}^{-1}$ , and almost no MO decomposition was observed for  $\text{K}_{0.58}\text{Sn}_{0.29}\text{TaWO}_6 \cdot 1.0\text{H}_2\text{O}$  under visible light irradiation. The stability of the photocatalyst has been verified by recording the PXRD pattern of the photocatalyst,  $\text{Sn}_{0.92}\text{Sb}_2\text{O}_6 \cdot 2.0\text{H}_2\text{O}$ , after MO decomposition under visible light irradiation (Supporting Information, Figure S6). It was very similar to the PXRD of the as prepared catalyst. We further investigated the rate of formation of active  $\cdot\text{OH}$  radicals under visible light irradiation as most of the photocatalytic degradation reactions involve the reaction of holes with surface adsorbed water and hydroxyl groups to produce reactive  $\cdot\text{OH}$  radicals.<sup>22–24</sup> Figure 7 shows the PL spectra of  $\text{Sn}_{0.92}\text{Sb}_2\text{O}_6 \cdot 2.0\text{H}_2\text{O}$  in TA solution at room

temperature under visible light irradiation. The PL intensity after light irradiation increased steadily, indicating the formation of the active  $\cdot\text{OH}$  species (Figure 7a). For comparison, the peak intensities are plotted with time in the dark and under visible light irradiation (Figure 7b). Similar experiments were carried out for  $\text{K}_{0.59}\text{Sn}_{0.20}\text{SbWO}_6 \cdot 1.0\text{H}_2\text{O}$  and  $\text{K}_{0.58}\text{Sn}_{0.29}\text{TaWO}_6 \cdot 1.0\text{H}_2\text{O}$ , and the corresponding fluorescent intensity plots with time (Figure 7b) show that the rate of formation of  $\cdot\text{OH}$  radicals were much slower than that of  $\text{Sn}_{0.92}\text{Sb}_2\text{O}_6 \cdot 2.0\text{H}_2\text{O}$ . The above results clearly suggested that the extent of degradation abilities of these oxides was consistent with the rate of formation of the active  $\cdot\text{OH}$  radicals under visible light irradiation. Finally, band structure calculations might suitably explain the positions of the valence and the conduction band levels of these  $\text{Sn}^{2+}$  pyrochlore oxides whose band gaps vary from 2.02 to 2.58 eV and also the possible mechanism for their photocatalytic properties.

#### 4. Conclusions

$\text{Sn}^{2+}$  incorporated pyrochlore type oxides were synthesized by simple ion-exchange reactions in aqueous tin(II) chloride solutions under ambient conditions oxides. The exchanged products,  $\text{Sn}_{0.92}\text{Sb}_2\text{O}_6 \cdot 2.0\text{H}_2\text{O}$ ,  $\text{K}_{0.59}\text{Sn}_{0.20}\text{SbWO}_6 \cdot 1.0\text{H}_2\text{O}$ , and  $\text{K}_{0.58}\text{Sn}_{0.29}\text{TaWO}_6 \cdot 1.0\text{H}_2\text{O}$  showed absorption in the visible region because of the reduction in their band gaps. The pseudo first order rate constants for the decomposition of aqueous MO solutions observed for the  $\text{Sn}^{2+}$  ion-exchanged oxides were  $1.34 \text{ h}^{-1}$  and  $0.217 \text{ h}^{-1}$  for  $\text{Sn}_{0.92}\text{Sb}_2\text{O}_6 \cdot 2.0\text{H}_2\text{O}$  and  $\text{K}_{0.59}\text{Sn}_{0.20}\text{SbWO}_6 \cdot 1.0\text{H}_2\text{O}$ , respectively, and almost negligible decomposition was noticed in the case of  $\text{K}_{0.58}\text{Sn}_{0.29}\text{TaWO}_6 \cdot 1.0\text{H}_2\text{O}$ . The observed rates of decomposition were found to be proportional to the rates of formation of active  $\cdot\text{OH}$  radicals as shown by the emission spectra of 2-hydroxyterephthalic acid.

**Acknowledgment.** The present research is supported by the Department of Science and Technology, Government of India. The authors also thank the University of Delhi for the financial support under the ‘‘Scheme to strengthen R & D Doctoral Research Programme’’. We thank Dr. R. Nagarajan, Department of Chemistry, University of Delhi

(32) Herrmann, J. M.; Tahiri, H.; Ait-Ichou, Y.; Lassaletta, G.; Gonzalez-Elipe, A. R.; Fernandez, A. *Appl. Catal., B* **1997**, *13*, 219.

(33) Lin, X.; Huang, F.; Wang, W.; Wang, Y.; Xia, Y.; Shi, J. *Appl. Catal., A* **2006**, *313*, 218.

for extending some of the experimental facilities and for constant support. We thank Dr. P. D. Sahare, Department of Physics, University of Delhi, for spectrofluorometer measurements. J.S. and V.T. thank UGC for their junior research fellowships.

**Supporting Information Available:** The TGA data for the parent pyrochlore-type oxides (Figure S1), SEM images of the

parent pyrochlore-type oxides and their  $\text{Sn}^{2+}$  exchanged pyrochlore-type oxides (Figures S2 and S3), the TGA for the  $\text{Sn}^{2+}$  exchanged pyrochlore-type oxides (Figure S4), the EDAX analysis data for the  $\text{Sn}^{2+}$  incorporated pyrochlore-type oxides (Figure S5), and PXRD patterns of the catalyst  $\text{Sn}_{0.92}\text{Sb}_2\text{O}_6 \cdot 2.0\text{H}_2\text{O}$  before and after MO decomposition under visible light irradiation (Figure 6). This material is available free of charge via the Internet at <http://pubs.acs.org>.